JNMS Journal of Nippon Medical School https://www.nms.ac.jp/sh/jnms/

Original

Placenta-Specific miRNA *miR-515-3p* Suppresses *HMGB3* Expression in the Breast Cancer Cell Line MCF-7

Ai Sato[1,2], Hiroyuki Takei[2], Syunya Noguchi[1] and Toshihiro Takizawa[1]

[1]Department of Molecular Medicine and Anatomy, Nippon Medical School, Tokyo, Japan
[2]Department of Breast Surgery and Oncology, Nippon Medical School, Tokyo, Japan

Background: Pregnancy-related breast cancer is relatively rare, but its incidence is increasing as the age of childbearing advances. The impact of placenta-specific microRNAs (miRNAs) derived from the chromosome 19 miRNA cluster (C19MC) on pregnancy-associated breast cancer is unclear. Nuclear protein high mobility group box 3 (HMGB3) plays a role in cancer progression. This study examined the effects of placenta-specific C19MC miRNAs on the cancer-related gene *HMGB3* in the human breast cancer cell line MCF-7.

Methods: We used target gene prediction programs to identify C19MC miRNAs that modulate *HMGB3* and then validated them using analytical procedures (i.e., quantitative PCR, Western blot, and luciferase reporter assay). We investigated how inhibition of *HMGB3* by C19MC miRNAs affects the invasive and proliferative ability of MCF-7 cells and explored the downstream effectors of this axis.

Results: C19MC miRNA *miR-515-3p* targeted *HMGB3*. In MCF-7 cells, reduction of *HMGB3* expression by *miR-515-3p* increased cell invasion and proliferation. Furthermore, *miR-515-3p*-mediated *HMGB3* inhibition led to the upregulation of CTNNB1 and GRB2, implicating invasion- and proliferation-related signaling pathways (e.g., WNT/β-catenin, Ras/MAPK, and PI3K/AKT/mTOR) in MCF-7 cells.

Conclusions: The impact of C19MC miRNA *miR-515-3p* on the cancer-related gene *HMGB3* in MCF-7 cells suggests a potential tumor-suppressive role for HMGB3 that contrasts with previous reports of oncogenic activity. The present findings raise the possibility that placenta-specific C19MC miRNAs play a role in pregnancy-related breast cancer during pregnancy.

(J Nippon Med Sch 2026; 93 (2): 122–134. https://doi.org/10.1272/jnms.JNMS.2026_93-206)

Keywords: C19MC microRNA, HMGB3, breast cancer, MCF-7

Introduction

Breast cancer accounts for 22.3% of all cancers among Japanese women and is the most frequent cancer site in women. Analysis of annual trends in breast cancer incidence rates by age group showed that the rate is high among women in their 40s and 50s[1]. Among adolescents and young adults (AYA) generation, who are typically 15 to 39 years of age at the time of diagnosis or care, breast cancer represents about 5% of all cases, but this rate starts to increase from the late 20s and is highest among those aged 35–39[1]. Pregnancy-related breast cancer (defined as breast cancer diagnosed during pregnancy, within the first year after childbirth, or during lactation) is relatively rare, but its incidence is increasing as the age of childbearing advances[2].

High mobility group box 3 (HMGB3) is a nuclear protein belonging to the HMGB protein family, which comprises four HMGB proteins (i.e., HMGB1–4)[3–5]. HMGB3 exhibits amino acid sequences analogous to those observed in HMGB1 and HMGB2 (~80% sequence identity).

Correspondence to Toshihiro Takizawa, t-takizawa@nms.ac.jp
https://doi.org/10.1272/jnms.JNMS.2026_93-206
Received: September 12, 2025; Accepted: November 12, 2025

HMGB3 contains two DNA-binding domains, thereby modulating DNA repair, replication, recombination, and transcription as well as gene expression. This multifunctional molecule plays a role in various cellular processes, including the immune response, inflammation, infection, and cancer progression[3–5]. Attention has focused on HMGB1 and HMGB2 because of their association with cancer, but reports have also linked HMGB3 to cancer, with high expression in a variety of cancers[3–5]. In the context of breast cancer, high HMGB3 expression promotes invasion and proliferation of breast cancer cells[6–8]. HMGB 3 has also been proposed as a potential indicator of unfavorable outcomes in breast cancer[9].

MicroRNAs (miRNAs) are a class of small noncoding RNA molecules that are about 22 nucleotides long[10]. They repress translation of target mRNAs via partial complementary sequences in their 3′-untranslated regions (3′-UTRs), thus contributing to various physiological cell functions and the molecular pathology of diseases[11]. In the context of cancer, dysregulation of miRNAs (abnormal expression of miRNAs targeting cancer-related genes) contributes to carcinogenesis and cancer progression[12]. It has been reported that the cancer-related gene *HMGB3* is modulated by deregulated miRNAs in cancers, including breast cancer[4]. While numerous miRNAs exhibit broad expression across multiple organs, despite variations in expression levels, certain miRNAs are predominantly expressed in specific tissues/organs[13,14]. The tissue-/organ-specific expression of miRNAs underlies their specialized regulatory roles in different tissues/organs (e.g., *miR-1*[15]). The placenta is not an exception in this regard; chromosome 19 miRNA cluster (C19MC)-derived miRNAs are placenta-specific miRNAs[16]. C19MC miRNAs are detected as early as 2 weeks after implantation, with their concentrations rising afterwards[17,18]. During pregnancy, placenta-specific miRNAs are released from villous trophoblast cells of the placenta into the maternal bloodstream, where they exert their influence on maternal cells[16,19]. However, the impact of placenta-specific C19MC miRNAs on pregnancy-associated breast cancer cells remains to be elucidated.

Using the breast cancer cell line MCF-7 to investigate the effects of placenta-specific C19MC miRNAs on the cancer-related gene *HMGB3* in breast cancer cells, we found that C19MC miRNA *miR-515-3p* targeted *HMGB3*. Moreover, whereas previous studies reported that *HMGB3* inhibition suppresses cancer cell invasion and proliferation, we observed that *miR-515-3p*-mediated *HMGB3* inhibition promoted cell invasion and proliferation in MCF-7 cells.

Materials and Methods

Culture

The E2-responsive MCF-7 human breast cancer cell line was obtained from the Cell Bank (ID TKG 0479, Cell Resource Center for Biomedical Research, Institute of Development, Aging and Cancer Tohoku University, Sendai, Japan). MCF-7 cells (passages 33–72) were maintained in RPMI-1640 medium (cat. no. 189-02025, Wako, Osaka, Japan) supplemented with 10% fetal bovine serum (FBS; cat. no. 10438, Gibco, USA) at 37°C under 5% CO_2.

Transfection of RNA Oligos

For miRNA transfection analysis, miRNA mimic oligos for *hsa-miR-515-3p*, *hsa-miR-519a-5p*, and *cel-miR-239b-5p* as a negative control miRNA (designated as miR-NC) were purchased from Ajinomoto Bio-Pharma (Osaka, Japan). For mRNA-knockdown analysis, the following small interfering RNA (siRNA) oligos were used: siRNA for *HMGB3* (designated as siHMGB3), sense: 5′-GUUGUCUUGUUUCUGUAUAUA-3′ and antisense: 5′-UAUACAGAAACAAGACAACCU-3′; siRNA for negative control (designated as siNC), sense: 5′-UUCUCCGAACGUGUCACGUTT-3′ and antisense: 5′-ACGUGACACGUUCGGAGAATT-3′ (Ajinomoto Bio-Pharma). Each miRNA and siRNA oligo (at final concentrations of 50 nM) was transfected into cells using Lipofectamine 2000 (cat. no. 11668019, Invitrogen, Waltham, MA, USA) at 37°C for 4 h.

Quantitative Polymerase Chain Reaction (qPCR)

Total RNA was isolated from the samples with RNAiso Plus (cat. no. 9109, Takara Bio, Shiga, Japan), according to the manufacturer's instructions. Then, qPCR was performed with the HT7900 FAST Real-Time PCR System (Applied Biosystems Waltham, MA, USA) according to the manufacturer's instructions. TB Green Premix Ex Taq (cat. no. RR420, Takara Bio) was used for the quantitative analysis of mRNA level. To normalize the expression level of mRNAs, 18S ribosomal RNA (designated as 18S) was used. The PCR assays were conducted three to five times under each experimental condition. The mRNA primers used in this investigation are listed in **Table 1**.

Western Blotting

Western blotting was performed as described previously[20]. Cell lysates were obtained using radioimmunoprecipitation (RIPA) lysis buffer: 50 nM Tris-HCl pH 7.5,

Table 1 Primer list for qPCR

Gene	Primer orientation (5′–3′)	Primer sequence
HMGB3	Forward (F)	TCCGCTTATGCCTTCTTTGTGC
	Reverse (R)	ATGCCGGGGTTTGTGGATTTG
HMGB1	F	TAAGAAGCCGAGAGGCAAAA
	R	CTCTTTCATAACGGGCCTTG
HMGB2	F	AGAAAAAGGACCCCAATGCT
	R	TGCTCAGACCACATTTCACC
CTNNB1	F	CTTACACCCACCATCCCACT
	R	GCACGAACAAGCAACTGAAC
MYC	F	TCCTCGGATTCTCTGCTCTC
	R	ACTCTGACCTTTTGCCAGGA
MMP2	F	TATGGCTTCTGCCCTGAGAC
	R	CACACCACATCTTTCCGTCA
MMP7	F	TGCTCACTTCGATGAGGATG
	R	GGGATCTCCATTTCCATAGGT
MMP9	F	TTGACAGCGACAAGAAGTGG
	R	CGGCACTGAGGAATGATCTAA
MMP14	F	TCCATCAACACTGCCTACGA
	R	TCCAGAAGAGAGCAGCATCA
GRB2	F	ACGATGGGGCCTTTCTTATC
	R	AACTTCACCACCCAGAGGAA
18S	F	AGTTGGTGGAGCGATTTGTC
	R	CGGACATCTAAGGGCATCAC

150 mM NaCl, 1% Triton X-100 (cat. no. X100-100 mL, Sigma-Aldrich, St. Louis, Missouri, USA), 1% deoxycholate (cat. no. 194-08311, FUJIFILM Wako Pure Chemical Corp., Osaka, Japan), 0.1% SDS (cat. no. 191-07145, FUJIFILM Wako Pure Chemical Corp.), and 1 mM PMSF (cat. no. ab141032, Abcam, Cambridge, UK) containing a Halt protease inhibitor cocktail (cat. no. 78430, Thermo Fisher Scientific). The lysates were sonicated three times and incubated on ice for 15 min. The lysates were cleared by centrifugation at 12,000 × *g* at 4°C for 5 min. Protein concentration was quantified using a TaKaRa BCA protein assay kit (cat. no. T9300A, Takara Bio). Three micrograms of the cell lysate protein was separated using Mini-PROTEAN TGX gels (4–20% gel: cat. no. 456-1094, Bio-Rad, Hercules, CA, USA) with a Model 200/2.0 power supply (100 V, 96 min; cat. no. 165-4761, Bio-Rad). The proteins were then transferred onto polyvinylidene fluoride membranes using Sequi-Blot PVDF membranes (cat. no. 162-0184, Bio-Rad) with a Trans-Blot SD Semi-Dry Electrophoretic Transfer Cell (cat. no. 1703940, Bio-Rad). Blotted proteins were incubated with primary antibodies (rabbit anti-HMGB3 [cat. no. 27465-1-AP, Proteintech, Rosemont, IL, USA], rabbit anti-CTNNB1 [cat. no. 9562, Cell Signaling, Danvers, MA, USA], mouse anti-GRB2 [cat. no. 610111, BD Transduction Laboratories, Franklin Lakes, NJ, USA], or mouse anti-GAPDH [cat. no. sc-32233, Santa Cruze, Dallas, TX, USA]) at 4°C overnight, followed by incubation with horseradish peroxidase-conjugated anti-mouse (cat. no. 115-035-003, Jackson ImmunoReserch, West Grove, PA, USA) or anti-rabbit (cat. no. 111-035-144, Jackson ImmunoReserch) secondary antibody at 22°C for 2 h. Signals were detected with an Amersham ECL Prime Western Blotting Detection Reagent (cat. no. RPN2232, GE Healthcare, Chicago, IL, USA) and visualized using an Amersham ImageQuant 800 OD Western blot imaging system (cat. no. 29399483, Cytiva, Tokyo, Japan). The Western blot assays were conducted three times under each experimental condition.

Cell Invasion Assay

The cell invasion assay was performed as described previously[21]. In brief, growth factor reduced BD Matrigel (cat. no. 356231, Corning, NY, USA) was coated onto cell culture inserts (Falcon Transparent polyethylene terephthalate [PET] Membrane/24 well, 8.0 µm pore size; cat. no. 353097, Corning). The Matrigel concentration was 200 µg/mL (2.2%). These upper chambers were set onto the lower chambers (Falcon 24-well TC-treated Cell Polystyrene Permeable Support Companion Plate; cat. no. 353504, Corning). MCF-7 cells were transfected with miRNA mimics or the siRNAs described above. After transfection for 24 h, the cells in 400 µL of each culture

medium without FBS were seeded in the upper chamber (1.5×10^5 cells/well). Then, 700 µL of each culture medium with 10% FBS was added to the lower chamber. After incubation for 6, 12, 24, or 48 h, the cells were fixed with 3% glutaraldehyde (cat. no. G003, TABB, Berkshire, UK)-PBS and stained with hematoxylin (cat. no. 131-09665, FUJIFILM Wako Pure Chemical Corp.). Noninvading cells at the top of each Transwell chamber were scraped off using cotton swabs. The invading cells at the bottom of the membrane were cut out with the membrane and sealed with CC/Mount (cat. no. K002, Diagnostic BioSystems, Harge, Netherlands) and counted manually using a light microscope (DFC7000T, Leica Microsystems, Wetzlar, Germany) under 200× magnification. The average numbers of invading cells in five areas were counted to reflect the invasive ability. The invasion assays were conducted three times under each experimental condition.

Cell Proliferation Assay

Evaluation of cell proliferation ability was performed using a Cell Counting Kit-8 (CCK-8) (cat. no. 341, Dojindo, Kumamoto, Japan). MCF-7 cells were transfected with miRNA mimics (50 nM) or siRNAs (50 nM) described above. After transfection for 24 h, 1.0×10^5 cells were seeded in 96-well plates. Following an additional incubation for 12, 24, or 48 h, 10 µL of CCK-8 was added per well and maintained at 37°C for 4 h. At 450 nm, the absorption values were measured using an iMerk microplate absorbance reader (Bio-Rad, CA, USA). The cell proliferation assay was measured three times for each experimental condition.

Luciferase Reporter Assay

The luciferase reporter assay was performed as described previously[21]. To construct a reporter plasmid, we first cloned the 3′-UTR of human *HMGB3* into the pMIR-REPORT vector (cat. no. AM5795, Applied Biosystems). Total RNA isolated from MCF-7 cells was reverse-transcribed to cDNA using PrimeScript reverse transcriptase (cat. no. 2680A, Takara Bio). The portion of the *HMGB3* 3′-UTR (2,857 nucleotides [nt]) including the target candidate sequence of *miR-515-3p* was then amplified from the cDNA with the following primers: GCCGAGCTCAGAAACTGTTTATCTGTCTCCTTG (*Sac*I site underlined) and GCCACGCGTTTTTTGGGAAGAGTGATTAAGA (*Mlu*I site underlined). After sequence verification, the *HMGB3* 3′-UTR (2,857 nt) was cloned into pMIR-REPORT via the *Sac*I and *Mlu*I restriction sites. This final construct was designated as pMIR-HMGB3/wild. To construct reporter plasmids with two predicted mutated *miR-515-3p* recognition sites (seed sequence pairing regions: nt 248–254 and nt 2,099–2,105 from the 5′ end) in the *HMGB3* 3′-UTR (**Figure 1C**), an inverse PCR method was used[22]. The primers used for the inverse PCR were as follows: HMGB3 3′-UTR-mutation 1, forward: gtgTTCTCCTcactctgtgc and reverse: gagGACATTCtttcatttaaaaatg (complementary sequence shown in lowercase); HMGB3 3′-UTR-mutation 2, forward: tccAGAATTTcccctcctg and reverse: acaGACATTCctgggcaaac (complementary sequence shown in lowercase). PCR amplification was performed using the previously cloned vector ZERO Blunt TOPO (cat. no. K280002, Thermo Fisher Scientific) containing the *HMGB 3* 3′-UTR. Plasmid DNA was digested by *Dpn*I. Amplified DNA was transformed into *Escherichia coli* (One Shot TOP10: cat. no. C404003, Thermo Fisher Scientific). After sequence verification, the two mutated 3′-UTR sequences were cloned into pMIR-REPORT via the *Sac*I and *Mlu*I restriction sites. Two final constructs for the *miR-515-3p* recognition sites (seed sequence pairing regions: nt 248–254 and nt 2,099–2,105) in the *HMGB3* 3′-UTR were designated as pMIR-HMGB3/mut1 and pMIR-HMGB3/mut2, respectively. In a manner analogous to the construction of the reporter plasmids with the predicted mutated *miR-515-3p* recognition sites in the *HMGB3* 3′-UTR, reporter plasmids with mutations introduced into two predicted *miR-519a-5p* recognition sites (seed sequence pairing regions: nt 145–152 and nt 2,049–2,055) were constructed (**Figure 1D**). The two final constructs for the *miR-519a-5p* recognition sites (seed sequence pairing regions: nt 145–152 and nt 2,049–2,055) in the *HMGB3* 3′-UTR were designated as pMIR-HMGB3/mut3 and pMIR-HMGB3/mut4, respectively (**Figure 1D**).

For the reporter assay, MCF-7 cells were transfected with these generated pMIR-REPORT vectors and the control vector pRL-TK (Renilla luciferase expression plasmid), together with 50 nM miRNA mimic using Lipofectamine 2000 in 24-well plates. At 24 h after transfection, luciferase assays were performed using the Dual Luciferase Reporter Assay System (cat. no. E1910, Promega, Madison, WI, USA). Firefly luciferase (from the pMIR-REPORT vector) and Renilla luciferase (from the phRL-TK vector) activities in the cell lysates were measured using the Glomax-Multi Detection System (Promega). Firefly luciferase activity was normalized to Renilla luciferase activity. The luciferase activity was measured three times for each experimental condition.

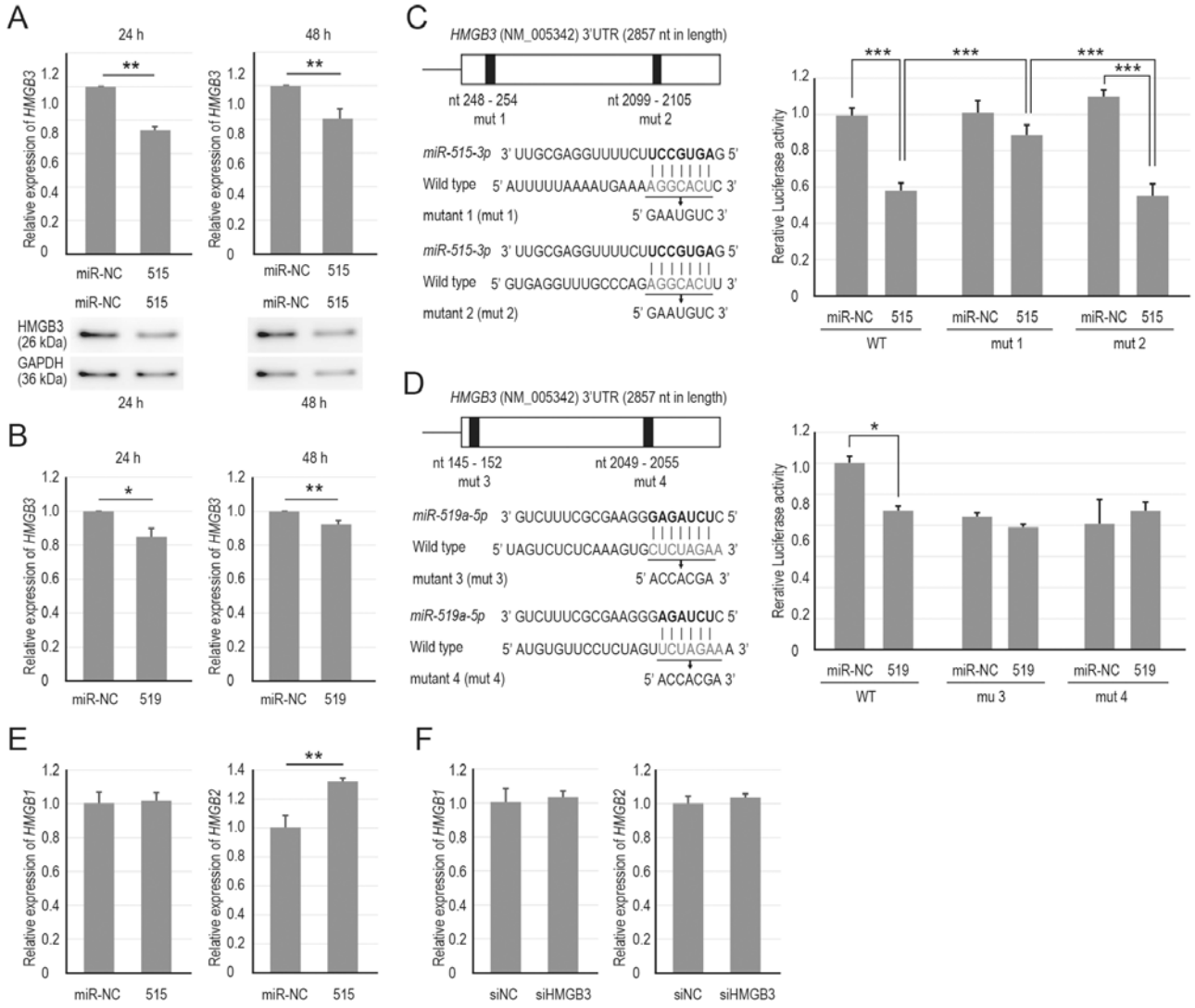

Figure 1 *miR-515-3p* targets *HMGB3* mRNA

(A) HMGB3 mRNA (upper panel) and protein (lower panel) expression in MCF-7 cells transfected with 50 nM miR-515-3p mimic (515) or cel-miR-239b-5p negative control mimic (miR-NC) and cultured for 24 h (left panel) and 48 h (right panel). (B) *HMGB3* mRNA expression in the cells transfected with 50 nM miR-519a-5 mimic (519) or miR-NC and cultured for 24 h (left panel) and 48 h (right panel). (C) *HMGB3* 3′ -UTR luciferase reporter assay for *miR-515-3p*. Sequences of the two putative target sites of *miR-515-3p* (seed sequence pairing regions: nt 248–254 and nt 2,099–2,105) that are represented by black areas in the schematic diagram of the 3′ -UTR of *HMGB3*; the mutations introduced into the *miR-515-3p* recognition sites of the 3′ -UTR (left panel). A reporter vector (pMIR-HMGB3/wild [WT], pMIR-HMGB3/mut1 [mut 1], or pMIR-HMGB3/mut2 [mut 2]) and miR mimic (50 nM 515 or miR-NC) were co-transfected into the cells (right panel). (D) *HMGB3* 3′ -UTR luciferase reporter assay for *miR-519a-5p*. Sequences of the two putative target sites of *miR-519a-5* (seed sequence pairing regions: nt 145–152 and nt 2,049–2,055) that are represented by black areas in the schematic diagram of the 3′ -UTR of *HMGB3*; the mutations introduced into the *miR-519a-5* recognition sites of the 3′ -UTR (left panel). A reporter vector (pMIR-HMGB3/wild [WT], pMIR-HMGB3/mut3 [mut 3], or pMIR-HMGB3/mut4 [mut 4]) and miR mimic (50 nM 519 or miR-NC) were co-transfected into the cells (right panel). (E) *HMGB1* and *HMGB2* mRNA expression in the cells transfected with 50 nM 515 or miR-NC and cultured for 48 h. (F) *HMGB1* and *HMGB2* mRNA expression in the cells transfected with 50 nM siHMGB3 or siNC and cultured for 48 h. In the qPCR assay, 18S was used for normalization; in Western blotting, GAPDH was used as the internal control; in the luciferase assay, the Renilla luciferase vector pRL-TK was utilized as the internal control. The Western blot data are representative images derived from the results of three independent experiments. qPCR data are expressed as the mean ± standard deviation (SD) of the results from three independent experiments. Student's *t*-test (A, B, E, and F) or Tukey's test (C and D) was used to assess between-group differences; $*p < 0.05$, $**p < 0.01$, $***p < 0.001$.

In Silico Prediction of miRNAs that Target *HMGB3* Gene

The sequences of miRNAs were obtained from the miRNA Registry miRbase[23]. The miRNAs that suppress *HMGB3* mRNA were predicted by several target gene prediction programs, consisting of TargetScanHuman database[24,25], miRmap[26,27], miRDB[28,29], miRWalk[30,31]. Expression levels of miRNAs in maternal plasma and placental tissues were searched using miRmine[32,33].

Statistics

Statistical analyses were conducted using the SPSS statistical software package (Windows version 20; IBM-SPSS, Chicago, IL, USA). The significance of between-group differences was assessed using Student's *t*-test or analysis of variance followed by Tukey's test, and *P*-values < 0.05 were considered to indicate statistical significance. Values are expressed as mean ± standard deviation (SD).

Results

In Silico Approach on Placenta-Specific miRNAs that Target *HMGB3* mRNA

First, we sought to identify placenta-specific C19MC miRNAs that potentially target *HMGB3* mRNA. To this end, we screened in silico-predicted *HMGB3*-targeting C19MC miRNAs and ranked candidate miRNAs based on the predicted strength of *HMGB3* suppression using four independent miRNA target prediction databases (**Table 2**). Among the top-ranked placenta-specific miRNA candidates, we focused on those sharing a common seed sequence (UCUAGAG) within the *HMGB3* 3′-UTR binding site, taking into account their reported abundance in maternal plasma and placental tissues according to the miRmine database (**Table 2**)[32,33]. Among these, *miR-519a-5p* was selected as the most abundant miRNA with the same mature sequence for further study. *miR-515-3p* was also selected as a candidate miRNA with a different seed sequence (AGUGCCU) for further study.

miR-515-3p Targets *HMGB3* mRNA

We performed qPCR to investigate whether *HMGB3* mRNA is downregulated by *miR-519a-5p* or *miR-515-3p* in MCF-7 cells. The expression of *HMGB3* mRNA was significantly downregulated in both miR-519a-5p mimic-transfected and miR-515-3p mimic-transfected cells compared with cells transfected with a negative control mimic (designated as miR-NC) (**Figure 1A and 1B**). Subsequently, we used a luciferase reporter assay to determine whether *miR-519a-5p* or *miR-515-3p* directly target *HMGB3* mRNA. Transfection of the miR-515-3p mimic led to a significant decrease in luciferase activity in MCF-7 cells co-transfected with pMIR-HMGB3/wild compared with that of miR-NC mimic (**Figure 1C**). Luciferase activity was unchanged in the cells transfected with pMIR-HMGB3/mut1, in which a potential *miR-515-3p* recognition site containing the seed sequence pairing region from nt 248 through 254 in the *HMGB3* 3′-UTR was mutated, whereas it was significantly reduced in the cells transfected with pMIR-HMGB3/mut2, in which another potential *miR-515-3p* recognition site containing the seed sequence pairing region from nt 2,099 through 2,105 in the *HMGB3* 3′-UTR was mutated (**Figure 1C**). These results indicate that *HMGB3* has the *miR-515-3p* binding site (seed sequence pairing region: nt 248–254) and is a direct target of *miR-515-3p*. In contrast, MCF-7 cells that were co-transfected with a miR-519a-5p mimic and either pMIR-HMGB3/mut3 or pMIR-HMGB3/mut4, luciferase activities were unrecoverable in the presence of mutated putative *miR-519a-5p* recognition sites in the *HMGB3* 3′-UTR, suggesting that *HMGB3* mRNA may be modulated indirectly via other target genes of *miR-519a-5p* (**Figure 1 D**). Thus, on the basis of the results of the luciferase assay, subsequent analyses focused on *miR-515-3p*.

We examined the protein level of HMGB3 in MCF-7 cells overexpressing *miR-515-3p* through Western blot analysis. As shown in **Figure 1A**, transfection of miR-515-3p mimic markedly downregulated the protein level of HMGB3 in the cells. Taken together, these results confirm that *HMBG3* is a target of *miR-515-3p.* Furthermore, with respect to *HMGB1* and *HMGB2*, which show a high degree of similarity in their amino acid sequences, overexpression of *miR-515-3p* or the siRNA suppression of *HMGB3* did not lead to suppression of their mRNA expression in MCF-7 cells (**Figure 1E and 1F**).

miR-515-3p Accelerates MCF-7 Cell Invasion and Proliferation

To investigate the effect of the inhibition of *HMBG3* by *miR-515-3p* on the invasive capacity of MCF-7 cells, an invasion assay was performed. miR-515-3p mimic-transfection significantly promoted the invasive capacity of the cells compared with miR-NC mimic-transfection (**Figure 2A**). To determine the role of *miR-515-3p*-induced *HMBG3* suppression in enhancing MCF-7 cell invasion, invasion by cells with *HMGB3* knockdown via siRNA was analyzed, where this siRNA was designated as siHMGB3 (**Figure 2B and 2C**). siHMGB3 efficiency was initially evaluated by qPCR and Western blotting (**Figure**

Table 2 In silico prediction of placenta-specific miRNAs that target *HMGB3* mRNA

			TargetScanHuman				miRmap	miRwalk	miRDB	miRmine	
No.	Mature miRNA	Seed sequence (underlined) from the 5′ end of miRNA	Context++ score percentile	1st position in the 3′-UTR	Context++ score percentile	2nd position in the 3′-UTR	Score	Score	Target score	Plasma[a]	Placenta[b]
1	*miR-518f-5p*	C**UCUAGAG**GGAAGCACUUUCUC	99	145–152	80	2,049–2,055	88.1	0.96	84	9	29
2	*miR-519a-5p*	C**UCUAGAG**GGAAGCGCUUUCUG	99	145–152	79	2,049–2,055	84.4	0.96	84	11	39
3	*miR-519b-5p*	C**UCUAGAG**GGAAGCGCUUUCUG	99	145–152	79	2,049–2,055	84.4	0.96	84	25	44
4	*miR-519c-5p*	C**UCUAGAG**GGAAGCGCUUUCUG	99	145–152	79	2,049–2,055	84.4	0.96	84	25	44
5	*miR-522-5p*	C**UCUAGAG**GGAAGCGCUUUCUG	99	145–152	79	2,049–2,055	84.4	0.96	84	25	44
6	*miR-523-5p*	C**UCUAGAG**GGAAGCGCUUUCUG	99	145–152	79	2,049–2,055	84.4	0.96	84	25	44
7	*miR-518e-5p*	C**UCUAGAG**GGAAGCGCUUUCUG	99	145–152	79	2,049–2,055	84.4	0.96	84	29	35
8	*miR-518d-5p*	C**UCUAGAG**GGAAGCACUUUCUG	99	145–152	80	2,049–2,055	87.6	0.96	84	37	51
9	*miR-520c-5p*	C**UCUAGAG**GGAAGCACUUUCUG	99	145–152	80	2,049–2,055	87.6	0.96	84	37	50
10	*miR-526a-5p*	C**UCUAGAG**GGAAGCACUUUCUG	99	145–152	80	2,049–2,055	87.6	0.96	84	N/A	
11	*miR-519e-3p*	A**AGUGCCU**CCUUUUAGAGUGUU	96	248–254	69	2,099–2,105	98.8	0.92	51	N/A	36
12	*miR-515-3p*	G**AGUGCCU**UCUUUUGGAGCGUU	95	248–254	71	2,099–2,105	98.9	0.92		7	17
13	*miR-520 g-5p*	U**CUAGAGG**AAGCACUUUCUGUUU	94	2,041–2,047	94	2,041–2,047		1.00		33	53
14	*miR-526b-3p*	G**AAAGUGC**UUCCUUUUAGAGGC	93	276–282			53.0	0.85	72	N/A	27
15	*miR-519d-3p*	C**AAAGUGC**CUCCCUUUAGAGUG	92	276–282			42.2	1.00	71	13	5
16	*miR-522-3p*	A**AAAUGGU**UCCCUUUAGAGUGU	92	1,700–1,706	53	1,493–1,499	93.7	0.85	59	24	20
17	*miR-520d-5p*	C**UACAAAG**GGAAGCCCUUUC	90	333–339	66	401–407	80.5		88	1	34

[a] The numerical values represent the order in which 47 C19MC miRNAs were ranked according to their detection levels in maternal plasma.

[b] The numerical values represent the order in which 56 C19MC miRNAs were ranked according to their detection levels in placental tissues.

N/A: not available.

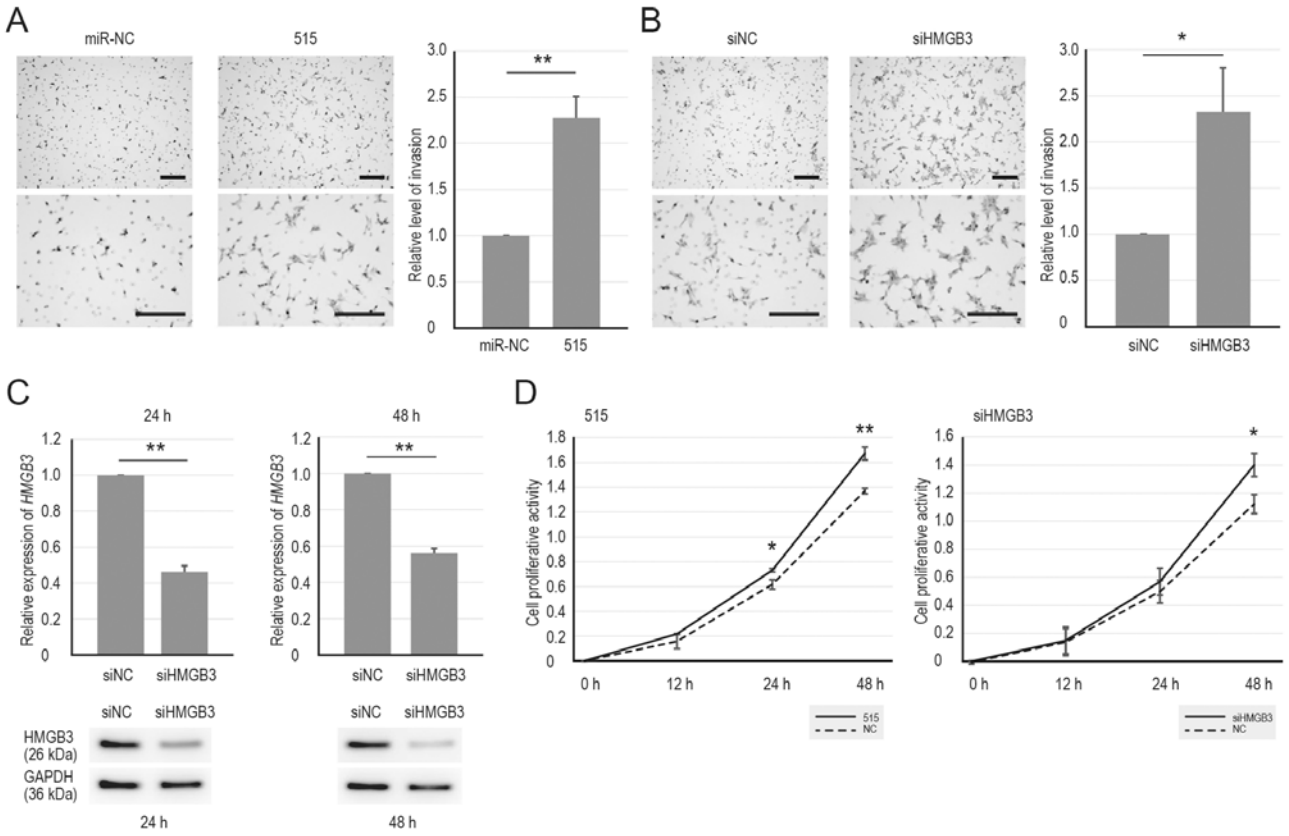

Figure 2 *miR-515-3p* accelerates MCF-7 cell invasion and proliferation
(A) Transwell invasion assay of MCF-7 cells transfected with miR-515-3p mimic (515) or negative control mimic (miR-NC). Representative images of the invasive MCF-7 cells (left panel). Quantification of the invasive cells per field (right panel). (B) Transwell invasion assay of the cells transfected with siRNA for *HMGB3* (siHMGB3) or negative control siRNA (siNC). Representative images of the invasive cells (left panel). Quantification of the invasive cells per field (right panel). (C) Knockdown efficiency in the cells transfected with siHMGB3. HMGB3 mRNA (upper panel) and protein (lower panel) expression in the cells transfected with 50 nM siHMGB3 or siNC and cultured for 24 h (left panel) and 48 h (right panel). (D) Cell proliferation (growth) assay. Left panel: MCF-7 cells transfected with 50 nM 515 (solid line) or miR-NC (dotted line). Right panel: the cells transfected with 50 nM siHMGB3 (solid line) or siNC (dotted line). In the qPCR assay, 18S was used for normalization; in Western blotting, GAPDH was used as the internal control. In the cell proliferation assay, cell proliferation was evaluated by measuring ATP activity at 24, 48, and 72 h after each oligo transfection. The transwell invasion, qPCR, and cell proliferation data are expressed as the mean ± SD of the results from three independent experiments. Student's *t*-test was used to assess between-group differences; *$p < 0.05$, **$p < 0.01$; bars = 200 μm.

2C). In MCF-7 cells, siHMGB3 significantly reduced expression of both HMGB3 mRNA and protein compared with negative control siRNA, designated as siNC, as depicted in **Figure 2C**. Invasion of cells that had been treated with siHMGB3 was then investigated. After siHMGB3 led to significant enhancement in the invasive capacity of the cells compared with the siNC (**Figure 2B**).

We further examined the effect of *miR-515-3p* transfection on the growth of MCF-7 cells. Transfection of a miR-515-3p mimic significantly increased cell proliferation compared with the miR-NC mimic (**Figure 2D**). In addition, siHMGB3 silencing significantly induced cell proliferation compared with siNC (**Figure 2D**). Taken together, these findings indicate that *miR-515-3p* has a positive regulatory effect on MCF-7 cell invasion and proliferation via induction of *HMBG3* inhibition.

miR-515-3p-mediated *HMGB3* Inhibition Upregulates CTNNB1 and GRB2

Subsequently, we investigated the downstream effectors modulated by the *miR-515-3p*/*HMGB3* axis in MCF-7 cell invasion and proliferation. In the context of HMBG3-mediated cancer invasion and proliferation, involvement of the WNT/β-catenin pathway has been reported in several cancers[34–36]. We therefore investigated gene expression changes in catenin beta 1 (CTNNB1), a transcriptional co-regulator in the WNT/β-catenin pathway, and its putative downstream signaling molecules (i.e., MYC proto-

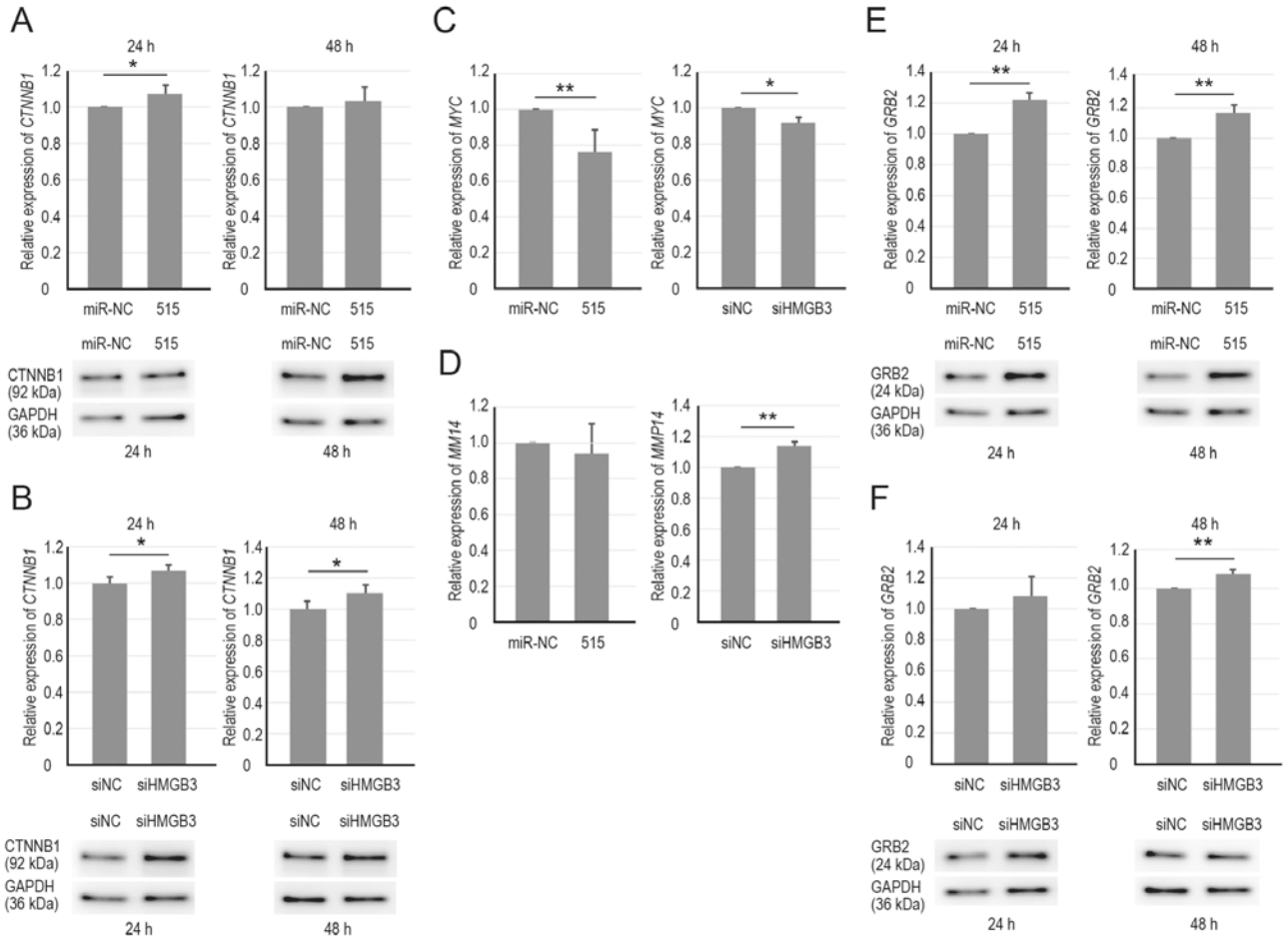

Figure 3 *miR-515-3p*-mediated *HMGB3* inhibition upregulates CTNNB1 and GRB2 in MCF-7 cells
(A) CTNNB1 mRNA (upper panel) and protein (lower panel) expression in MCF-7 cells transfected with 50 nM miR-515-3p mimic (515) or cel-miR-239b-5p negative control mimic (miR-NC) and cultured for 24 h (left panel) and 48 h (right panel). (B) CTNNB1 mRNA (upper panel) and protein (lower panel) expression in the cells transfected with 50 nM siRNA for *HMGB3* (siHMGB3) or negative control siRNA (siNC) and cultured for 24 h (left panel) and 48 h (right panel). (C) *MYC* mRNA expression in the cells transfected with 50 nM 515 or miR-NC (left panel) and in those transfected with 50 nM siHMGB3 or siNC (right panel), after 48 h of culture. (D) *MMP14 mRNA* expression in the cells transfected with 50 nM 515 or miR-NC (left panel) and in those transfected with 50 nM siHMGB3 or siNC (right panel), after 48 h of culture. (E) GRB2 mRNA (upper panel) and protein (lower panel) expression in the cells transfected with 515 or miR-NC and cultured for 24 h (left panel) and 48 h (right panel). (F) GRB2 mRNA (upper panel) and protein (lower panel) expression in the cells transfected with 50 nM siHMGB3 or siNC and cultured for 24 h (left panel) and 48 h (right panel). In the qPCR assay, 18S was used for normalization; GAPDH was used as the internal control for Western blotting. The Western blot data are representative images derived from the results of three independent experiments. The qPCR data from 515-transfection are expressed as the mean ± SD of the results from five independent experiments. With the exception of *CTNB1*, derived from the qPCR data of five independent experiments in siHMGB3-transfection, the qPCR data for the remaining genes were based on three independent experiments. Student's *t*-test was used to assess between-group differences; *$p < 0.05$, **$p < 0.01$.

oncogene, bHLH transcription factor [MYC], Matrix Metallopeptidase 2 [MMP2]), MMP7, MMP9, and MMP14)[37], following transfection of MCF-7 cells with a miR-515-3p mimic or siHMGB3.

To evaluate whether CTNNB1 is altered in miR-515-3p mimic-transfected or siHMGB3-transfected cells compared with control cells, we used qPCR and Western blotting to examine their CTNNB1 expression levels. Both miR-515-3p mimic and siHMGB3 treatments significantly upregulated both the mRNA and protein levels of CTNNB1 (**Figure 3A and 3B**). Subsequently, qPCR was conducted to identify changes in the gene expression of the five candidate downstream signaling molecules of β-catenin mentioned above. Both the miR-515-3p mimic and siHMGB3 treatments significantly reduced *MYC* mRNA expression in MCF-7 cells (**Figure 3C**). However, neither the miR-515-3p mimic nor siHMGB3 treatment led to an increase in *MMP2* and *MMP9* expression levels

(data not shown). *MMP7* mRNA was undetectable in MCF-7 cells. miR-515-3p mimic administration had no effect on *MMP14* expression, whereas siHMGB3 transfection caused a significant increase in its expression (**Figure 3D**).

Subsets of breast cancer cells possess receptor tyrosine kinase (RTK) family members, including human epidermal growth factor receptor 2 (HER2)[38]. Upon activation of these RTKs, the recruitment of growth factor receptor bound protein 2 (GRB2) occurs, subsequently activating downstream signaling pathways, including the Ras/MAPK and PI3K/AKT/mTOR pathways[39,40]. These pathways differ from the WNT/β-catenin pathway but also enable cancer cell proliferation, survival, invasion, and metastasis. GRB2 functions as a central hub within these signaling pathways. Thus, we attempted to evaluate whether GRB2 is altered in miR-515-3p mimic-transfected or siHMGB3-transfected cells compared with control cells, and investigated their expression levels of GRB2 using qPCR and Western blotting. Both the miR-515-3p mimic and siHMGB3 treatments significantly upregulated both the mRNA and protein levels of GRB2 (**Figure 3E and 3F**). These results suggest that GRB2 is upregulated through *miR-515-3p*-mediated *HMGB3* suppression.

Discussion

To date, there have been no reports on how placenta-specific miRNAs circulating in maternal blood affect breast cancer cells during pregnancy. In this study, we used the breast cancer cell line MCF-7 to investigate the effect of placenta-specific miRNAs on the invasion and proliferation of breast cancer cells. Our findings demonstrated that *miR-515-3p* targeted *HMGB3* and promoted MCF-7 cell invasion and proliferation via induction of *HMGB3* inhibition. Furthermore, we found that *miR-515-3p*-mediated reduction of *HMGB3* was accompanied by increased expression of CTNNB1 and GRB2, which are potential downstream effectors in the *miR-515-3p/HMGB3* axis, implicating invasion- and proliferation-related signaling pathways (e.g., WNT/β-catenin, Ras/MAPK, and PI3K/AKT/mTOR) in MCF-7 cells.

Previous studies have shown that in several cancer cells high expression of HMGB3 triggers activation of CTNNB1, a key downstream effector in the WNT/β-catenin pathway; this activation then sets off a chain reaction in downstream signaling molecules such as MYC and MMPs, ultimately leading to increased cell invasion and proliferation[34–36]. Although non-C19MC miRNAs (e.g., *miR-205*) and HIF1A have been reported as regulators associated with elevated HMGB3 expression in breast cancer cells, no studies to date have identified the WNT/β-catenin pathway as a downstream signaling axis mediating HMGB3-driven cell invasion and proliferation induced by these molecules[6–8,41]. Additionally, high HMGB3 expression is a documented clinical factor associated with enhanced breast cancer cell invasion and proliferation, for which the downstream signaling mechanisms responsible for these effects remain undefined[9,42]. Although CTNNB1, the main downstream effector of the WNT/β-catenin pathway, appears to be involved in MCF-7 breast cancer cell invasion and proliferation modulated by the *miR-515-3p/HMGB3* axis, our findings imply a potential tumor-suppressive role for HMGB3, in contrast to previous reports[6–9,41,42].

The incongruity between present and previous findings may be attributable to differences in the subtypes of breast cancer cell lines used in the studies. Four main breast cancer subtypes are widely recognized: luminal A and B types, HER2-type, and triple-negative type[43,44]. However, comparison of present and previous findings on luminal A subtype MCF-7 cells also demonstrated an incongruity on HMGB3[7,42]. This discrepancy may be partially attributed to the possibility that miRNAs targeting *HMGB3* also affect paralog *HMGB1* and *HMGB2*. The previous studies have not documented the effects of *HMGB3*-targeted miRNAs on *HMGB1* and *HMGB2*. Our study showed that *miR-515-3p* had no effect on *HMGB1* expression but upregulated *HMGB2*, which may affect cell invasion and proliferation in *miR-515-3p*-transfected MCF-7 cells (**Figure 1E**). Other potential explanations for the observed inconsistency include influences on the invasion and proliferation of MCF-7 cells from other *miR-515-3p*-targeted genes, or effects from variations in E2 concentration in the culture medium. Further functional analysis of HMGB3 in MCF-7 cells is required in order to elucidate its role in this process. This study failed to conclusively show that downstream signaling molecules linked to HMGB3-mediated cell growth were indeed activated. CTNNB1 activates MYC, thereby promoting cell growth and proliferation[45–47]. In contrast, in the present study, the *CTNNB1* gene was upregulated via the *miR-515-3p/HMGB3* axis in MCF-7 cells, but *MYC* gene expression was repressed (**Figure 3C**). MYC suppression could be considered a rational downstream signal for promoting MCF-7 invasion. It has been reported that MYC has a suppressive effect on cancer cell migration and invasion[48,49]. In addition, MYC functions as an antimigratory agent in MCF-7 cells[50]. Therefore, suppression

of *MYC* via the *miR-515-3p*/HMGB3 axis may contribute to the promotion of MCF-7 invasion.

GRB2 is a crucial adapter molecule that has a key role in RTK signaling. RTKs, which are cell surface receptors that have a strong affinity for growth factors, cytokines, and hormones, control cancer cell proliferation, survival, metastasis, and angiogenesis[39,40]. Abnormal activation of these receptors is a primary factor in cancer development and progression. RTKs have been demonstrated to activate downstream signaling pathways, including the Ras/MAPK pathway and the PI3K/Akt/mTOR pathway, through the SHC-GRB2-SOS complex[39,40]. This activation has been linked to cellular processes like proliferation, survival, and cell migration. In breast cancer, especially in RTK family HER2-positive breast cancer cells, HER2 activation is crucial in promoting cell growth, survival, and metastasis via the aforementioned downstream signaling pathways[51]. The present findings on the modification of GRB2 by HMGB3 may offer a novel perspective on the role of HMGB3 in cancer development and metastasis. The unresolved molecular mechanism by which HMGB3 inhibits GRB2 also necessitates clarification on which downstream signaling pathways are subsequently activated after GRB2 upregulation in MCF-7 cells.

Current breast cancer treatment guidelines indicate that the prognosis for breast cancer during lactation is poor (Evidence Grade: Probable), yet the same cannot be definitively stated for breast cancer during pregnancy[52]. This study showed that placenta-specific C19MC miRNA *miR-515-3p* promoted invasion and proliferation of the luminal-type breast cancer cell line MCF-7 via *HMGB3* suppression. However, in the absence of further evidence, caution is warranted when interpreting this finding as contributing to a poor prognosis in vivo (in pregnant women with pregnancy-associated breast cancer). The complication in this context arises from the presence of 59 distinct mature C19MC miRNAs, variable detection levels in maternal blood, and the diverse capacity of individual C19MC miRNAs to target cancer-related mRNAs, alongside the intricate interaction between miRNAs and mRNAs, where not all C19MC miRNAs cause breast cancer invasion and proliferation unidirectionally. The present study examined the effect of a single placenta-specific C19MC miRNA (i.e., *miR-515-3p*) on a single breast cancer cell line (i.e., MCF-7). However, further analysis using maternal blood must attempt to clarify the impact on invasion and proliferation of different subtypes of breast cancer cell lines and the cells that are isolated and subsequently cultured from surgically excised breast cancer specimens, given the abundant, diverse placenta-specific C19MC miRNAs (mixture of mature miRNAs derived from forty-six C19MC pre-miRNAs) in maternal blood samples. This approach is distinct from analysis of a single C19MC miRNA and can be regarded as an in vivo experiment. This question remains unanswered.

In summary, we demonstrated that placenta-specific C19MC miRNA *miR-515-3p* targeted *HMGB3*. Our observations yielded contradictory results: *miR-515-3p*-mediated *HMGB3* suppression increased cell invasion and proliferation in the MCF-7 breast cancer cell line, contrary to previous studies suggesting that *HMGB3* suppression hinders cancer cell invasion and proliferation. Although further research is required in order to explore how placenta-derived C19MC miRNAs in maternal blood influence breast cancer cells in relation to breast cancer treatment during pregnancy, the present findings provide insight into the potential impact of placenta-specific miRNAs on pregnancy-related breast cancer.

Author Contributions: T.T. conceived and designed the experiments; H.T. and T.T. acquired the fundings; A.S. and S.N. performed the experimental analysis; A.S., S.N., and T.T. analyzed the data; H.T. and T.T. interpreted the data; T.T. drafted the manuscript. All authors have read and approved the final manuscript.

Acknowledgments: The authors wish to express their gratitude to Takuji Kosuge (Department of Molecular Medicine and Anatomy, Nippon Medical School) for his outstanding technical support.

Funding: This work was supported by the Grants-in-Aid for Scientific Research (Nos. 18K08583 and 22K07218 to H.T., and Nos. 17K11256 and 20K09611 to T.T.) from the Ministry of Education, Culture, Sports, Science and Technology (MEXT)/Japan Society for the Promotion of Science, Japan, and by the Nippon Medical School Grants-in-Aid for Medical Research to H.T. and T.T.

Conflict of Interest: The authors declare no conflicts of interest.

Declaration of Generative AI and AI-Assisted Technologies in the Writing Process: This manuscript was proofread using AI-based grammar checkers to improve its grammar and clarity. The manuscript is free of plagiarism, including any text or images generated by AI, and the authors take responsibility

for its content.

References

1. National Cancer Center Japan. [Cancer statistics by type: Breast] [Internet]. 2016 Apr 18. [cited 2025 May 27]. Available from: https://ganjoho.jp/reg_stat/statistics/stat/cancer/14_breast.html. Japanese.
2. Han SN, Van Calsteren K, Heyns L, Mhallem Gziri M, Amant F. Breast cancer during pregnancy: a literature review. Minerva Ginecol. 2010 Dec;62(6):585–97.
3. Chikhirzhina E, Tsimokha A, Tomilin AN, Polyanichko A. Structure and functions of HMGB3 protein. Int J Mol Sci. 2024 Jul 12;25(14):7656.
4. Wen B, Wei YT, Zhao K. The role of high mobility group protein B3 (HMGB3) in tumor proliferation and drug resistance. Mol Cell Biochem. 2021 Apr;476(4):1729–39.
5. Niu L, Yang W, Duan L, et al. Biological functions and theranostic potential of HMGB family members in human cancers. Ther Adv Med Oncol. 2020 Nov 10;12: 1758835920970850.
6. Gu J, Xu T, Huang QH, Zhang CM, Chen HY. HMGB3 silence inhibits breast cancer cell proliferation and tumor growth by interacting with hypoxia-inducible factor 1α. Cancer Manag Res. 2019 May 31;11:5075–89.
7. Sharma P, Yadav P, Sundaram S, Venkatraman G, Bera AK, Karunagaran D. HMGB3 inhibition by miR-142-3p/sh-RNA modulates autophagy and induces apoptosis via ROS accumulation and mitochondrial dysfunction and reduces the tumorigenic potential of human breast cancer cells. Life Sci. 2022 Sep 1;304:120727.
8. Elgamal OA, Park JK, Gusev Y, et al. Tumor suppressive function of mir-205 in breast cancer is linked to HMGB3 regulation. PLoS One. 2013 Oct 2;8(10):e76402.
9. Zhou X, Zhang Q, Liang G, Liang X, Luo B. Overexpression of HMGB3 and its prognostic value in breast cancer. Front Oncol. 2022 Dec 22;12:1048921.
10. Bartel DP. MicroRNAs: target recognition and regulatory functions. Cell. 2009 Jan 23;136(2):215–33.
11. Esteller M. Non-coding RNAs in human disease. Nat Rev Genet. 2011 Nov 18;12(12):861–74.
12. Croce CM. Causes and consequences of microRNA dysregulation in cancer. Nat Rev Genet. 2009 Oct;10(10):704–14.
13. Landgraf P, Rusu M, Sheridan R, et al. A mammalian microRNA expression atlas based on small RNA library sequencing. Cell. 2007 Jun 29;129(7):1401–14.
14. Rishik S, Hirsch P, Grandke F, Fehlmann T, Keller A. miRNATissueAtlas 2025: an update to the uniformly processed and annotated human and mouse non-coding RNA tissue atlas. Nucleic Acids Res. 2025 Jan 6;53(D1): D129–37.
15. Safa A, Bahroudi Z, Shoorei H, et al. miR-1: a comprehensive review of its role in normal development and diverse disorders. Biomed Pharmacother. 2020 Dec;132:110903.
16. Mouillet JF, Ouyang Y, Coyne CB, Sadovsky Y. Micro RNAs in placental health and disease. Am J Obstet Gynecol. 2015 Oct;213(4 Suppl):S163–72.
17. Dumont TMF, Mouillet JF, Bayer A, et al. The expression level of C19MC miRNAs in early pregnancy and in response to viral infection. Placenta. 2017 May;53:23–9.
18. Miura K, Miura S, Yamasaki K, et al. Identification of pregnancy-associated microRNAs in maternal plasma. Clin Chem. 2010 Nov;56(11):1767–71.
19. Luo SS, Ishibashi O, Ishikawa G, et al. Human villous trophoblasts express and secrete placenta-specific micro RNAs into maternal circulation via exosomes. Biol Reprod. 2009 Oct;81(4):717–29.
20. Noguchi S, Tozawa S, Sakurai T, et al. BeWo exomeres are enriched for bioactive extracellular placenta-specific C19 MC miRNAs. J Reprod Immunol. 2024 Feb;161:104187.
21. Ogoyama M, Ohkuchi A, Takahashi H, Zhao D, Matsubara S, Takizawa T. LncRNA H19-derived miR-675-5p accelerates the invasion of extravillous trophoblast cells by inhibiting GATA2 and subsequently activating matrix metalloproteinases. Int J Mol Sci. 2021 Jan 27;22(3):1237.
22. Kambe S, Yoshitake H, Yuge K, et al. Human exosomal placenta-associated miR-517a-3p modulates the expression of PRKG1 mRNA in Jurkat cells. Biol Reprod. 2014 Nov;91(5):129.
23. University of Manchester. Homo sapiens miRNAs [Internet]. Manchester (GB): University of Manchester; 2006. [cited 2021 Oct 23]. Available from: https://www.mirbase.org/browse/results/?organism=hsa
24. Agarwal V, Bell GW, Nam JW, Bartel DP. Predicting effective microRNA target sites in mammalian mRNAs. Elife [Internet]. 2015 Aug 12;4:e05005. Available from: https://pubmed.ncbi.nlm.nih.gov/26267216
25. Whitehead Institute for Biomedical Research. Search for predicted microRNA targets in mammals [Internet]. Cambridge (GB): Whitehead Institute for Biomedical Research; 2006. [cited 2021 Oct 23]. Available from: https://www.targetscan.org/vert_72
26. Vejnar CE, Zdobnov EM. MiRmap: comprehensive prediction of microRNA target repression strength. Nucleic Acids Res [Internet]. 2012 Dec;40(22):11673–83. Available from: https://www.ncbi.nlm.nih.gov/pubmed/23034802
27. Vejnar CE, Zdobnov EM. miRmap: comprehensive prediction of microRNA target repression strength. Nucleic Acids Res [Internet]. 2012 Dec 1 [cited 2021 Oct 23];40(22): 11673–83. Available from: https://academic.oup.com/nar/article/40/22/11673/1146893?login=true
28. Chen Y, Wang X. miRDB: an online database for prediction of functional microRNA targets. Nucleic Acids Res [Internet]. 2020 Jan 8;48(D1):D127–31. Available from: https://www.ncbi.nlm.nih.gov/pubmed/31504780
29. miRDB Target Search [Internet]. [place unknown]: miRDB;. [cited 2021 Oct 23]. Available from: https://mirdb.org/index.html
30. Sticht C, De La Torre C, Parveen A, Gretz N. miRWalk: an online resource for prediction of microRNA binding sites. PLoS One [Internet]. 2018 Oct 18;13(10):e0206239. Available from: https://www.ncbi.nlm.nih.gov/pubmed/30335862
31. miRWalk Team. Search for a single gene or miRNA [Internet]. Mannheim: Medical Faculty Mannheim (DE), Heidelberg University; 2018. [cited 2021 Oct 23]. Available from: http://mirwalk.umm.uni-heidelberg.de
32. Panwar B, Omenn GS, Guan Y. miRmine: a database of human miRNA expression profiles. Bioinformatics [Internet]. 2017 May 15;33(10):1554–60. Available from: https://www.ncbi.nlm.nih.gov/pubmed/28108447
33. University of Michigan. miRmine - Human miRNA Expression Database [Internet]. Ann Arbor (MI): University of Michigan; 2017. [cited 2021 Oct 18]. Available from: http://bioconductor.riken.jp/packages/3.16/bioc/html/miRmine.html
34. Zhang Z, Chang Y, Zhang J, et al. HMGB3 promotes growth and migration in colorectal cancer by regulating WNT/β-catenin pathway. PLoS One. 2017 Jul 5;12(7):

e0179741.
35. Zhuang S, Yu X, Lu M, Li Y, Ding N, Ding Y. High mobility group box 3 promotes cervical cancer proliferation by regulating Wnt/β-catenin pathway. J Gynecol Oncol. 2020 Nov;31(6):e91.
36. Gong W, Guo Y, Yuan H, et al. HMGB3 is a potential therapeutic target by affecting the migration and proliferation of colorectal cancer. Front Cell Dev Biol. 2022 May 31;10:891482.
37. Ji Y, Lv J, Sun D, Huang Y. Therapeutic strategies targeting Wnt/β-catenin signaling for colorectal cancer (Review). Int J Mol Med. 2022 Jan;49(1):1.
38. Butti R, Das S, Gunasekaran VP, Yadav AS, Kumar D, Kundu GC. Receptor tyrosine kinases (RTKs) in breast cancer: signaling, therapeutic implications and challenges. Mol Cancer. 2018 Feb 19;17(1):34.
39. Luo LY, Hahn WC. Oncogenic signaling adaptor proteins. J Genet Genomics. 2015 Oct 20;42(10):521–9.
40. Regad T. Targeting RTK signaling pathways in cancer. Cancers (Basel). 2015 Sep 3;7(3):1758–84.
41. Li X, Wu Y, Liu A, Tang X. MiR-27b is epigenetically downregulated in tamoxifen resistant breast cancer cells due to promoter methylation and regulates tamoxifen sensitivity by targeting HMGB3. Biochem Biophys Res Commun. 2016 Sep 2;477(4):768–73.
42. Aljohani AI, Alsaeed SA, Toss MS, Raafat SA, Green AR, Rakha EA. The expression of high mobility group protein 3 (HMGB3) in breast cancer with emphasis on its role in lymphovascular invasion. Am J Cancer Res. 2023 Nov 15; 13(11):5334–51.
43. Sharma MP, Shukla S, Misra G. Recent advances in breast cancer cell line research. Int J Cancer. 2024 May 15;154 (10):1683–93.
44. Dai X, Cheng H, Bai Z, Li J. Breast cancer cell line classification and its relevance with breast tumor subtyping. J Cancer. 2017 Sep 12;8(16):3131–41.
45. Xu J, Chen Y, Olopade OI. MYC and breast cancer. Genes Cancer. 2010 Jun;1(6):629–40.
46. Fallah Y, Brundage J, Allegakoen P, Shajahan-Haq AN. MYC-driven pathways in breast cancer subtypes. Biomolecules. 2017 Jul 11;7(3):53.
47. Xu J, Chen Y, Huo D, et al. β-catenin regulates c-Myc and CDKN1A expression in breast cancer cells. Mol Carcinog. 2016 May;55(5):431–9.
48. Liu H, Radisky DC, Yang D, et al. MYC suppresses cancer metastasis by direct transcriptional silencing of αv and β3 integrin subunits. Nat Cell Biol. 2012 May 13;14 (6):567–74.
49. Ma X, Huang J, Tian Y, et al. Myc suppresses tumor invasion and cell migration by inhibiting JNK signaling. Oncogene. 2017 Jun 1;36(22):3159–67.
50. Cappellen D, Schlange T, Bauer M, Maurer F, Hynes NE. Novel c-MYC target genes mediate differential effects on cell proliferation and migration. EMBO Rep. 2007 Jan;8(1): 70–6.
51. Schlam I, Swain SM. HER2-positive breast cancer and tyrosine kinase inhibitors: the time is now. NPJ Breast Cancer. 2021 May 20;7(1):56.
52. Japanese Breast Cancer Society. [Breast Cancer Treatment Guidelines 2022 Edition] [Internet]. Tokyo: Japanese Breast Cancer Society; 2022 Nov 15. [BQ (Background Question) 18: Is breast cancer during pregnancy or lactation associated with poor prognosis?];. [cited 2025 May 27]. Available from: https://jbcs.xsrv.jp/guideline/2022/e_index/bq18. Japanese.